



## Research Article

<https://doi.org/10.1631/jzus.B2300880>



# Aberrant network topological structure of sensorimotor superficial white-matter system in major depressive disorder

Peng WANG<sup>1,2,3\*</sup>, Yanling BAI<sup>4\*</sup>, Yang XIAO<sup>5</sup>, Yuhong ZHENG<sup>1,2,3</sup>, Li SUN<sup>1,2,3</sup>, The DIRECT Consortium, Jinhui WANG<sup>6</sup>, Shaowei XUE<sup>1,2,3</sup>✉

<sup>1</sup>Center for Cognition and Brain Disorders / Department of Neurology, The Affiliated Hospital of Hangzhou Normal University, Hangzhou 311121, China

<sup>2</sup>Institute of Psychological Science, Hangzhou Normal University, Hangzhou 311121, China

<sup>3</sup>Zhejiang Key Laboratory for Research in Assessment of Cognitive Impairments, Hangzhou 311121, China

<sup>4</sup>Jing Hengyi School of Education, Hangzhou Normal University, Hangzhou 311121, China

<sup>5</sup>Institute of Mental Health, Peking University Sixth Hospital, Peking University, Beijing 100191, China

<sup>6</sup>Institute for Brain Research and Rehabilitation, South China Normal University, Guangzhou 510631, China

**Abstract:** White-matter tracts play a pivotal role in transmitting sensory and motor information, facilitating interhemispheric communication and integrating different brain regions. Meanwhile, sensorimotor disturbance is a common symptom in patients with major depressive disorder (MDD). However, the role of aberrant sensorimotor white-matter system in MDD remains largely unknown. Herein, we investigated the topological structure alterations of white-matter morphological brain networks in 233 MDD patients versus 257 matched healthy controls (HCs) from the DIRECT consortium. White-matter networks were derived from magnetic resonance imaging (MRI) data by combining voxel-based morphometry (VBM) and three-dimensional discrete wavelet transform (3D-DWT) approaches. Support vector machine (SVM) analysis was performed to discriminate MDD patients from HCs. The results indicated that the network topological changes in node degree, node efficiency, and node betweenness were mainly located in the sensorimotor superficial white-matter system in MDD. Using network nodal topological properties as classification features, the SVM model could effectively distinguish MDD patients from HCs. These findings provide new evidence to highlight the importance of the sensorimotor system in brain mechanisms underlying MDD from a new perspective of white-matter morphological network.

**Key words:** Major depressive disorder (MDD); Magnetic resonance imaging (MRI); White matter; Brain network

## 1 Introduction

Major depressive disorder (MDD) is a common psychiatric condition characterized by a persistent low mood and/or decreased interest (anhedonia), accompanied by feelings of worthlessness, guilt, and hopelessness, as well as unexplained physical anomalies (Malhi and Mann, 2018). Although no well-established brain mechanism has reasonably explained these

symptoms and disease etiology, MDD patients have consistently been reported to have structural and functional alterations in brain areas and circuits (Zhang et al., 2018). With the development and application of neuroimaging techniques and modern network theory (Petersen and Sporns, 2015), MDD has increasingly been conceptualized as a brain network disorder (Bassett and Sporns, 2017). Furthermore, MDD symptoms arise from network topological changes (Li et al., 2020). Previous studies have highlighted the disruption of topological properties of large-scale brain networks under the MDD condition based on global metrics such as global and local efficiencies, as well as nodal metrics including degree and betweenness (Li et al., 2021; Yang et al., 2021). For instance, a previous study reported a negative correlation between the characteristic path length and the rate of decrease in 24-item Hamilton

✉ Shaowei XUE, xuedrm@126.com

\* The two authors contributed equally to this work

Shaowei XUE, <https://orcid.org/0000-0001-5441-4522>

Peng WANG, <https://orcid.org/0009-0007-9204-0606>

Yanling BAI, <https://orcid.org/0009-0001-0013-3853>

Received Dec. 6, 2023; Revision accepted Apr. 19, 2024;  
Crosschecked Oct. 21, 2024; Published online Dec. 6, 2024

© Zhejiang University Press 2024

depression rating scale (HAMD-24) scores after an 8-week antidepressant treatment in MDD (Zhang et al., 2021). Another study found alterations in the topological features of dynamic brain networks in MDD, specifically a significant decrease in the variability of clustering coefficient in the frontal cortex, parietal cortex, and thalamus in individuals with MDD (Zhou et al., 2024). These brain network studies on altered topological properties somewhat broaden our insights into clinical diagnosis and treatment options.

The human brain is segmented into three tissue types: gray matter (GM), white matter (WM), and cerebrospinal fluid (CSF). WM is made up of bunches of myelinated axons of interconnecting neurons, forming distributed neural networks (Fields, 2010). Given that WM densely connects various GM regions and comprises approximately half the volume of the human brain, many previous researchers have focused on the topological changes of WM networks in normal and clinical populations, such as MDD patients (Sampaio-Baptista and Johansen-Berg, 2017). Magnetic resonance imaging (MRI) is a noninvasive neuroimaging technique to map the anatomical structures, physiological functions, and tissues of brain in vivo, while voxel-based morphometry (VBM), a widely adaptable analytical method, has been used for measuring voxel-level volume/concentration of brain tissues such as GM and WM (Whitwell, 2009). Previous MRI-based brain network studies mainly focused on the organization patterns between GM regions (Power et al., 2011; Yeo et al., 2011). However, there is accumulating evidence that blood oxygen level-dependent (BOLD) signals, detected in resting-state functional MRI (rs-fMRI), can be reliably detected in WM, and they dynamically fluctuate in a coordinated manner (Peer et al., 2017). For example, robust correlations have been observed between rs-fMRI signals from specific cortical GM regions and those from segmented WM tracts (Wang P et al., 2022).

Structural network connectivity can be mainly assessed via diffusion-weighted tractography to reconstruct axonal tracts between WM regions. Most WM structural networks are based on diffusion tensor imaging (DTI), whereas DTI has been surrounded by several controversies, such as the presence of false-positive connections (Aydogan et al., 2018), sensitivity to noise during image acquisition, such as head motion (Baum et al., 2018), and uncertainty in quantifying long-distance connections (Schilling et al., 2019).

Previous evidence from microscale biology and macroscopic brain imaging studies suggests that the morphological similarity of brain regions can, to some extent, infer structural connectivity (Meinertzhagen, 2018; Seidlitz et al., 2018). For example, a study tested whether large-scale structural reorganization in schizophrenia was related to normative network architecture, particularly to regional centrality/centrality and connectivity patterns, and suggested that schizophrenia was associated with widespread alterations in brain morphology and might be shaped by underlying connectome structures (Georgiadis et al., 2024). Based on these findings, it was hypothesized that axonal morphology can be applied to indirectly study structural connectivity between WM regions (Li et al., 2023). The morphology-informed analysis of structural connectivity may be particularly suited for WM regions due to their relatively homogeneous cellular composition, consisting of oligodendrocytes and astrocytes.

WM tracts are generally considered to play a pivotal role in transmitting sensory and motor information, facilitating interhemispheric communication and connecting various cortical regions (Wang et al., 2016). A growing body of research shows that MDD patients exhibit concurrent changes and gradients in both low-level sensorimotor and higher-order cognitive processing (Xiao et al., 2023). On the other hand, it was previously indicated that a diverse range of sensorimotor stimulation could modulate depressive symptoms (Canbeyli, 2013). Some studies have also suggested that MDD might lead to disruptions in the sensory perception system, and conversely, these disruptions in auditory and visual functions might be preclinical signs of depression (Lu et al., 2020). A meta-analysis found reduced regional homogeneity (ReHo) of the sensorimotor network in MDD patients, which is thought to involve psychomotor retardation (Iwabuchi et al., 2015). Sensorimotor-related brain regions could complement brain mechanisms underlying MDD to some extent and might also serve as target areas in antidepressant therapy involving transcranial magnetic stimulation. Nevertheless, extant research in this domain is limited, prompting the need for a comprehensive understanding of the sensorimotor signal patterns in MDD.

In the present study, we investigated the topological properties of individual WM morphological networks derived from VBM data using the three-dimensional discrete wavelet transform (3D-DWT) approach. Considering that sensorimotor changes have

been shown to be significantly involved in MDD, we hypothesized that aberrant network topological structure in the sensorimotor WM system would apparently mark MDD-related brain changes and might also discriminate MDD patients from normal controls. This study has great potential to highlight the clinical significance of the sensorimotor system in understanding the potential pathological mechanisms of MDD from the new perspective of WM network.

## 2 Materials and methods

### 2.1 Participants

The dataset analyzed in the present study consisted of 233 MDD patients and 257 healthy controls (HCs), as shown in Table 1. Participants were drawn from a publicly available dataset contributed by the six study sites (Sites 1, 2, 6, 7, 8, and 14) of the REST-meta-MDD project (Yan et al., 2019) from the DIRECT consortium (Chen et al., 2022). During screening, participants in the REST-meta-MDD consortium were first excluded if they: (1) had no information on gender, age, or education; (2) were aged < 18 years or >65 years; (3) had no information on the sub-item scores of the 17-item Hamilton depression rating scale (HAMD-17). Furthermore, we excluded stations with fewer than ten MDD patients or ten HC subjects to balance the subjects for optimizing the overall sample size and keeping extreme bias to a minimum. MDD patients were also excluded if they achieved a HAMD-17 score of <8 points. The primary approach for the diagnosis of MDD used operational diagnostic criteria in the Diagnostic and Statistical Manual of Mental Disorders IV.

### 2.2 White-matter network construction by three-dimensional discrete wavelet transform

The WM morphological network was constructed by mapping inter-regional similarities based on regional

morphology (i.e., WM volume) derived from structural MRI data. In this study, the nodes of the WM morphological network were randomly generated anatomical nodes based on WM volume, totaling 128 nodes. Connectivity was defined as the Pearson correlation coefficient of the wavelet feature vectors of regions of each node. The raw anatomical MRI data were pre-processed based on the standard procedure of VBM using Data Processing & Analysis of Brain Imaging (DPABI) software (<http://www.rfmri.org>). The T1 images were first segmented into GM, WM, and CSF in their original space, and the WM images were subsequently modulated and spatially normalized using the Diffeomorphic Anatomical Registration Through Exponentiated Lie (DARTEL) toolbox (Ashburner, 2007). The normalized images were modulated by multiplying the Jacobean determinants derived from previous DARTEL spatial normalization.

Wavelet transformation is a multiscale analysis method that transforms the energy of a signal into hierarchically organized levels of resolution, allowing the capture of both local and global features of anatomical MRI datasets. In this study, 3D-DWT was applied to the voxel-wise WM volume using the waverec3 function in MATLAB (Wang XH et al., 2022). Each voxel was decomposed into three different levels, and each level was further divided into high-pass and low-pass components. As a result, six (3×2) wavelet features were generated based on the volume of each voxel. An average WM structural mask across all participants was segmented into 128 contiguous anatomical regions (128 network nodes) across the whole brain using the region-growing method reported by Zalesky et al. (2010). The average wavelet feature vector of all voxels within each node was defined as the regional wavelet feature vector. The WM morphological similarity matrix (128×128) of each subject was obtained using the Pearson correlation coefficient between each pair of regional wavelet feature vectors, and then normalized using Fisher's  $r$  to  $z$

**Table 1 Demographic and clinical characteristics**

Group	Age (years)	Gender (male/female)	Education level (years)	HAMD-17 score
MDD ( $n=233$ )	34.738±11.170	78/155	12.223±3.709	23.537±5.439
HC ( $n=257$ )	33.883±11.295	105/152	13.973±3.526	
$t/\chi^2$	0.842	2.844	-5.338	
$P$	0.400	0.092	0.001	

Data are expressed as mean±standard deviation except gender. HAMD-17: 17-item Hamilton depression rating scale; MDD: major depressive disorder; HC: healthy control.

transformation. Follow-up analysis of network topological properties was performed based on the weighted WM similarity matrix. A schematic analysis of individual WM morphological networks is shown in Fig. 1.

### 2.3 Graph theory analysis of white-matter networks

The graph theory analysis of WM networks was performed using GREYNA software (Wang et al., 2015). We calculated the network topological properties over a range of network sparsity thresholds (from 5% to 40%, with 1% step size) for each individual weighted matrix. The global properties included clustering coefficient ( $C_p$ ), characteristic path length

( $L_p$ ), normalized clustering coefficient ( $\gamma$ ), normalized characteristic path length ( $\lambda$ ), global efficiency ( $E_{\text{glob}}$ ), local efficiency ( $E_{\text{loc}}$ ), and small-worldness ( $\sigma$ ). The nodal properties included node efficiency, node degree, and node betweenness. Some global properties were further normalized using the corresponding average of 100 matched random networks, generated by a topological rewiring algorithm to maintain the same degree distribution as the real networks (Maslov and Sneppen, 2002). Small-world WM networks have global properties ( $\gamma > 1$  and  $\lambda \approx 1$ , or  $\delta = \gamma/\lambda > 1$ ) that indicate relatively high local interconnectivity and an approximately equivalent shortest path length compared with random networks (Liao et al., 2017).

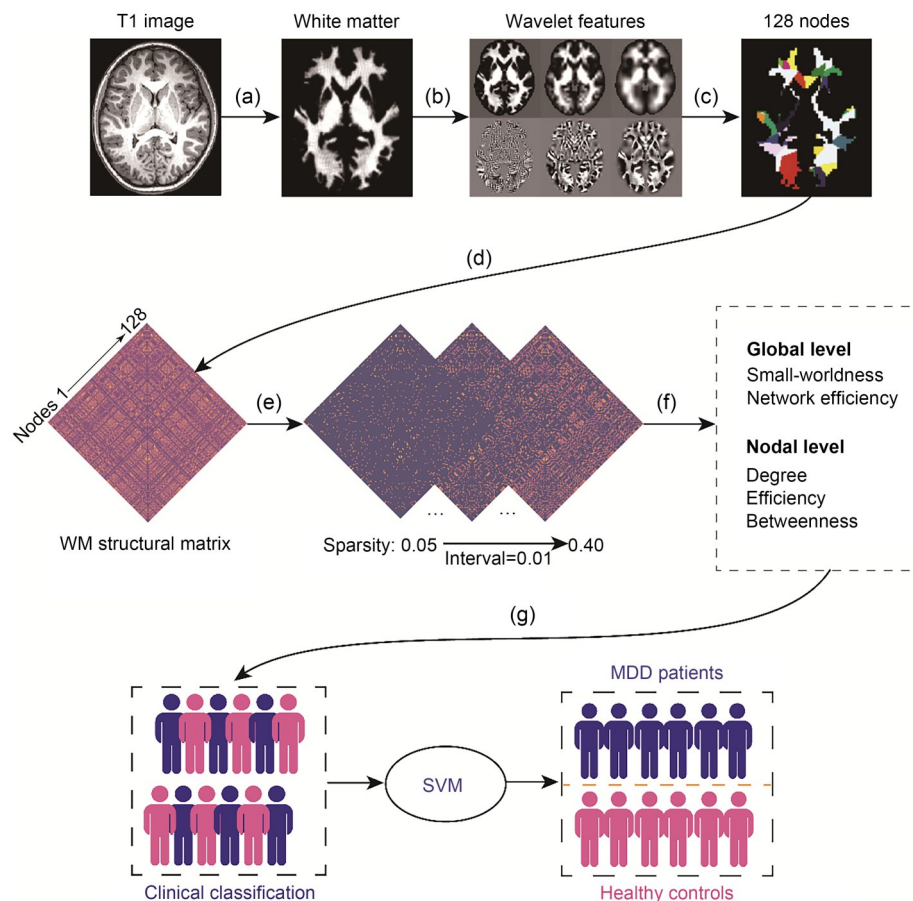


**Fig. 1** Flowchart for the construction and analysis of individual white-matter (WM) morphological networks. (a) For each subject, voxel-based morphology (VBM) transform was performed on the spatially normalized and modulated T1-weighted WM images. (b) Three-dimensional (3D) wavelet transform was performed on the individual VBM volume. (c) The group-level WM mask was randomly separated into 128 anatomical nodes of approximately identical size. The WM was assigned to 128 nodes. (d) Interregional morphological similarity was computed based on the correlation coefficients of the node's wavelet features. (e) WM morphological networks were constructed across a series of sparsities from 0.05–0.40 (interval=0.01). (f) The area under the curve (AUC) values of topological properties (i.e., small-world topology and nodal topological properties) were then evaluated across a series of sparsity values. (g) The support vector machine model was used to classify major depressive disorder (MDD) patients and healthy controls. SVM: support vector machine.



The small-worldness of a complex network is described by its  $C_p$  and  $L_p$  values, where  $C_p$  refers to the number of edges between a node's nearest neighbors and indexes network segregation, and  $L_p$  represents the average shortest path length between all pairs of nodes in the network, which reflects the degree of network integration (Li et al., 2021).  $E_{\text{glob}}$  in the brain network is defined as "a measure of the overall capacity for parallel information transfer and integrated processing" (Bullmore and Sporns, 2012). These topological properties are known to be interrelated, with each providing a different viewpoint from which the major features of the large-scale architecture can be discerned (Zhang et al., 2011). The three nodal metrics selected in this study are among the most commonly utilized indicators in previous research. Nodal topological properties typically measure local information transfer efficiency, and alterations in nodal efficiency are considered to be associated with cognitive inhibitory deficits and depressive states (Li et al., 2021). To examine the distribution of nodes and between-group differences in nodal topological properties at the network level, we mapped the nodes with between-group differences ( $P < 0.05$ , false discovery rate (FDR) corrected) onto the defined 12 WM networks. The ComBat harmonization models were implemented to remove the confounding effects introduced by the site effects, with age, gender, and diagnosis as covariates (Fortin et al., 2018).

## 2.4 Statistical analysis

The two-sample  $t$ -test was applied to analyze the between-group differences of demographic and clinical data. The Chi-square test was used to measure gender differences between the MDD and HC groups. The global and nodal topological properties were compared between MDD and HC using non-parametric Mann-Whitney  $U$  tests, with age, gender, education, and head movement as covariates. Head movement, quantified using framewise displacement (FD) derived from the subjects' fMRI scans, was considered in light of prior research demonstrating the potential impact of in-scanner head motion on morphometric measures (Alexander-Bloch et al., 2016; Pardoe and Martin, 2022). The threshold of statistical significance was set at 0.05, corrected for multiple comparisons with an FDR method ( $P < 0.05$ , FDR corrected). We mapped network nodes with significant differences to 12 WM

networks according to previous high-quality research (Peer et al., 2017) (Table 2). The Pearson correlation coefficients between the topological properties and HAMD scores were calculated in the MDD group. The FDR correction was applied separately to between-group comparisons of global topological properties, local topological properties, and network-level topological properties, with a threshold set at  $P < 0.05$  for each type. Finally, we used support vector machine (SVM) classification models based on the area under the curve (AUC) values of global and nodal topological properties to distinguish between MDD and HC, and applied 5-fold cross-validation to the models.

**Table 2 White-matter networks**

Network label	Network name
1	Cingulum and associated tracts
2	Uncinate and middle temporal lobe tracts
3	Sensorimotor superficial white-matter system
4	Forceps minor system
5	Superior longitudinal fasciculus system
6	Visual superficial white-matter system
7	Inferior longitudinal fasciculus system
8	Inferior corticospinal tract
9	Posterior cerebellar tracts
10	Dorsal frontoparietal tracts
11	Deep frontal white matter
12	Ventral frontoparietal tracts

## 2.5 Classification model based on the topological properties of white-matter morphological network

To study the clinical application of the topological properties of the constructed WM structural network, we used an SVM model with a linear kernel function in Python's scikit-learn (<https://scikit-learn.org>) to distinguish MDD patients from HCs. The AUC values of global topological attributes (including  $\gamma$ ,  $\lambda$ ,  $\sigma$ ,  $C_p$ ,  $L_p$ ,  $E_{\text{glob}}$ , and  $E_{\text{loc}}$ ) and nodal topological attributes (including node degree, node efficiency, and node betweenness of 128 nodes) of each patient were used as classification features. We finally created two classification models, that is, the SVM classification model based on global topological properties and that based on nodal topological properties. We employed 5-fold cross-validation to the SVM classification model, with the outputs of accuracy and the AUC value of the receiver operating characteristic (ROC) curve for each

fold as evaluation metrics for the classification model. Finally, to illustrate the ultimate classification performance, we computed the average AUC value and accuracy for each model.

### 3 Results

#### 3.1 Between-group differences of network global topological properties

Figs. 2a and 2b present the comparison results of AUC values of global network properties. Compared with HCs, MDD patients showed a statistically significant increase in  $\sigma$  (Mann-Whitney  $U$  test,  $Z=2.60$ ,  $P=0.009$ , FDR corrected) and a decrease in  $L_p$  (Mann-Whitney  $U$  test,  $Z=-2.67$ ,  $P=0.007$ , FDR corrected). The other global network properties ( $\lambda$ ,  $\gamma$ ,  $C_p$ ,  $E_{glob}$ , and  $E_{loc}$ ) showed no significant between-group differences ( $P>0.05$ ). No significant correlations were found

between the two indicators ( $\sigma$  and  $L_p$ ) and the HAMD scores ( $P>0.05$ ; Fig. 2c).

#### 3.2 Between-group differences of network nodal topological properties

As shown in the left half of Fig. 3, MDD patients exhibited 30, 37, and 18 network nodes with significant differences ( $P<0.05$ , FDR corrected) in node degree, node efficiency, and node betweenness compared with HC, respectively. To examine the distribution of nodes on each network, we separately summarized the number of nodes with significant differences in each of the 12 networks, as shown in the right half of Fig. 3. Network 3, described as the sensorimotor superficial WM system (Table 2), had the maximum number of nodes with between-group differences (right half of Fig. 3; node degree: 9; node efficiency: 10; node betweenness: 7). There were no significant correlations between these indicators and HAMD scores ( $P>0.05$ ).

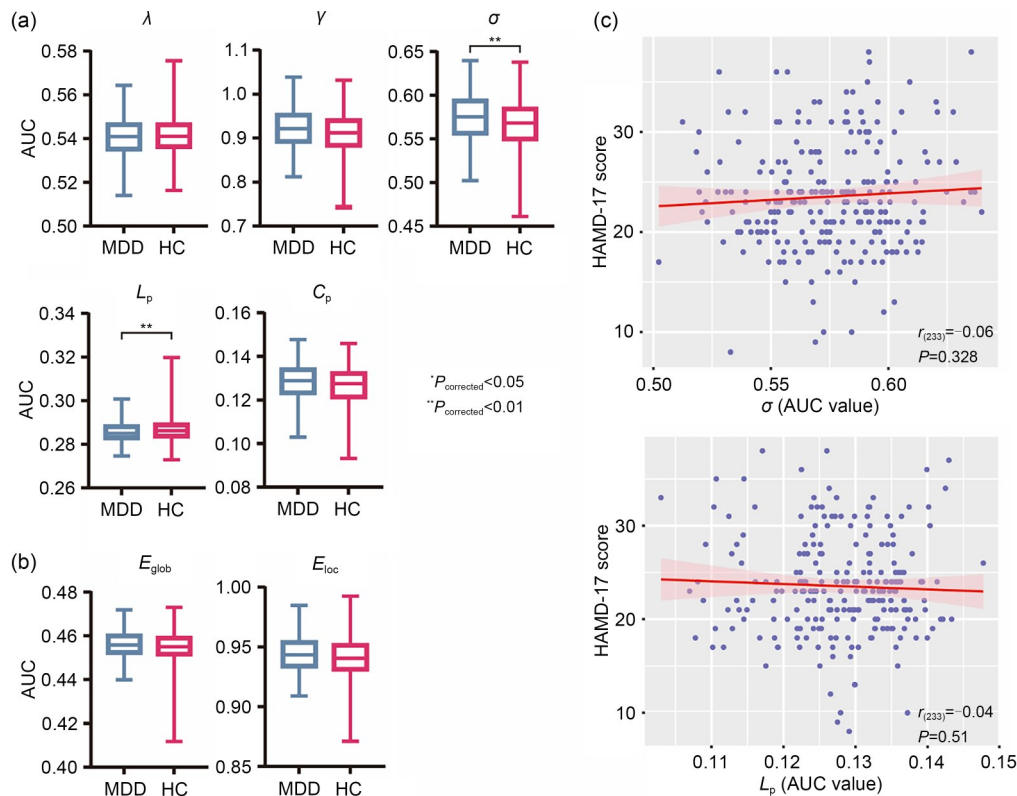


**Fig. 2** Between-group differences of network global topological properties. (a) Group comparison of global topological properties:  $\sigma$  and  $L_p$  showed significant differences, while  $\lambda$ ,  $\gamma$ , or  $C_p$  did not exhibit significant differences. (b) Group comparison of global efficiency and local efficiency: neither property showed significant differences between groups. (c) Correlation analyses of  $\sigma$  and  $L_p$  with HAMD-17 scores, revealing no significant correlations. MDD: major depressive disorder; HC: healthy control;  $\lambda$ : normalized characteristic path length;  $\gamma$ : normalized clustering coefficient;  $\sigma$ : small-worldness;  $L_p$ : characteristic path length;  $C_p$ : clustering coefficient;  $E_{glob}$ : global efficiency;  $E_{loc}$ : local efficiency; AUC: area under curve; HAMD-17: 17-item Hamilton depression rating scale.

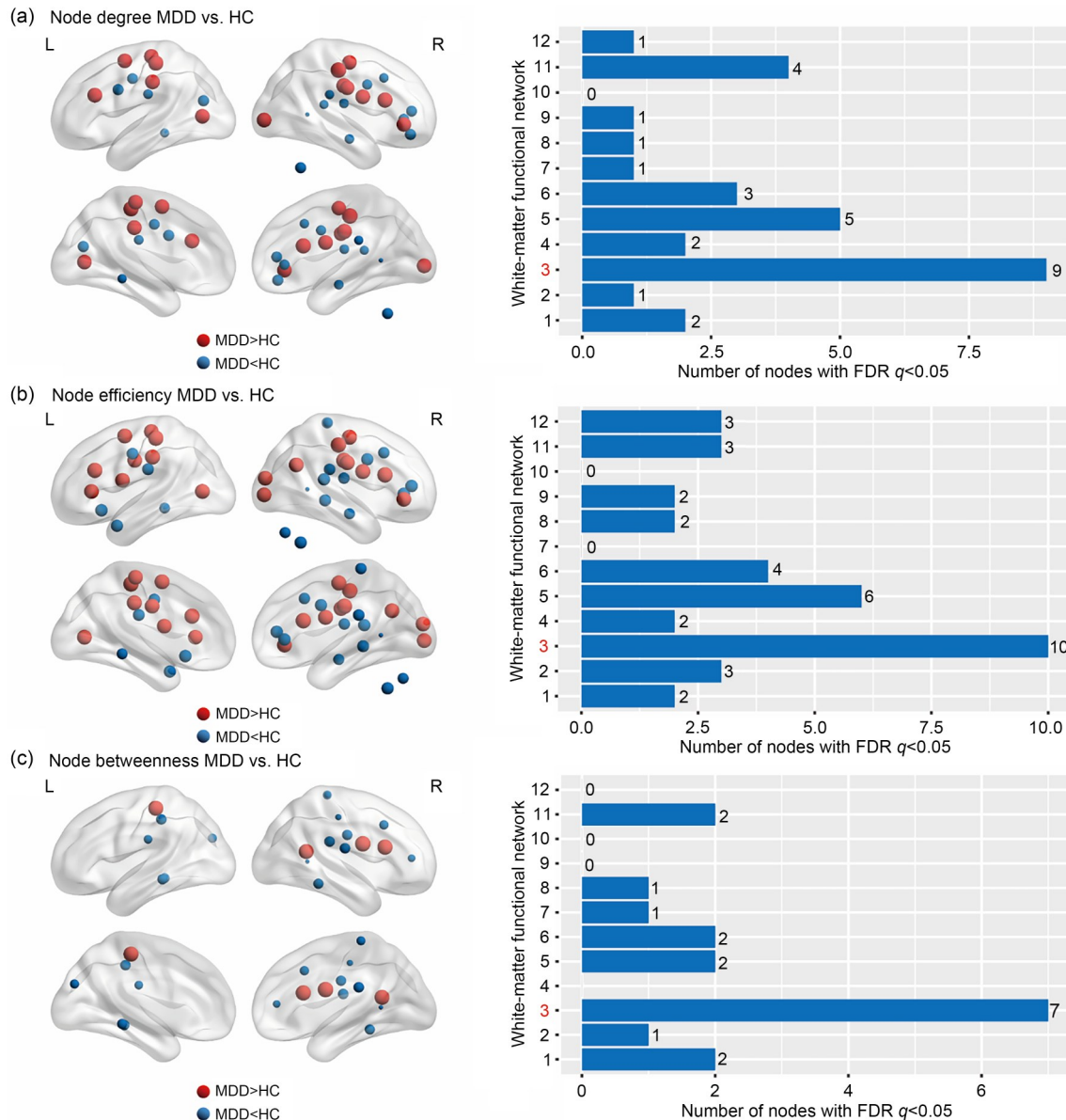


**Fig. 3** Between-group differences of network nodal topological properties. (a) Left: group comparison of the number of nodes with significant differences in node degree. Right: the number of nodes with significant differences in each network. (b) Left: group comparison of the number of nodes with significant differences in node efficiency. Right: the number of nodes with significant differences in each network. (c) Left: group comparison of the number of nodes with significant differences in node betweenness. Right: the number of nodes with significant differences in each network. The balls indicate significant between-group differences in the nodal topological properties ( $P < 0.05$ ), where red and blue balls denote increase and decrease in major depressive disorder (MDD) patients compared to healthy control (HC) subjects, respectively. The sphere size represents the significance of the difference (the  $Z$  value of the statistical test). FDR: false discovery rate.

As shown in Fig. 4, MDD patients showed statistically significant increases in the AUC values of node degree ( $Z = 4.48$ ,  $P < 0.001$ , FDR corrected) and node efficiency ( $Z = 3.76$ ,  $P = 0.002$ , FDR corrected) and decreases in the AUC values of node betweenness ( $Z = -3.12$ ,  $P = 0.011$ , FDR corrected), mainly in the

sensorimotor superficial WM system (Network 3) compared with HC. Besides, we found that MDD patients exhibited significant decreases in the AUC values of node degree ( $Z = -3.80$ ,  $P < 0.001$ , FDR corrected) and node betweenness ( $Z = -3.22$ ,  $P = 0.015$ , FDR corrected) in Network 1, node efficiency ( $Z = -2.76$ ,  $P = 0.035$ ,

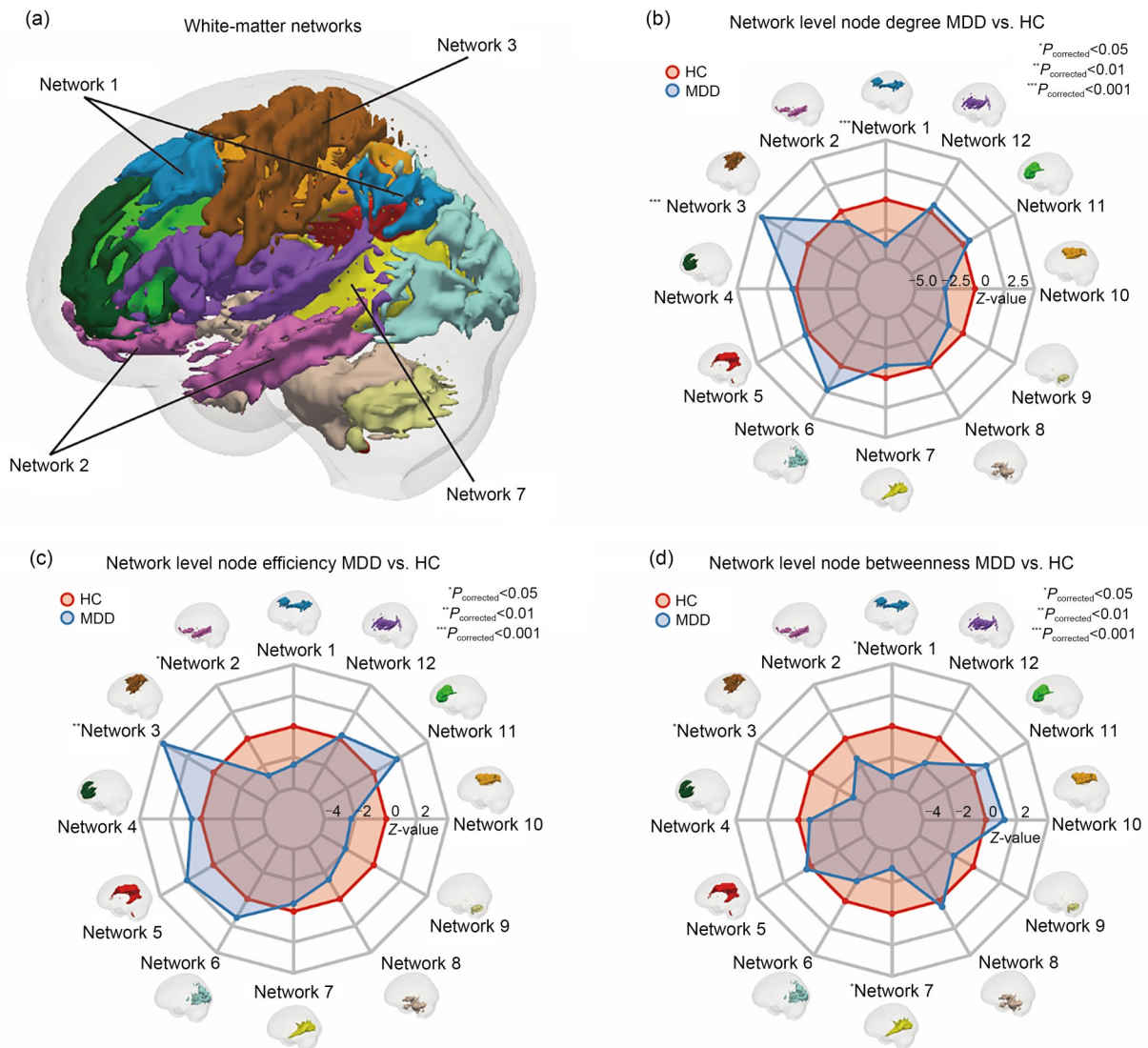


**Fig. 4** Between-group comparison of nodal topologies in 12 white-matter networks. The white-matter networks were defined by Peer's 12 white-matter network parcellation atlas. (a) The names and locations of networks with significant inter-group differences; (b) Distribution of group differences in AUC values for node degree across 12 networks; (c) Distribution of group differences in AUC values for node efficiency across 12 networks; (d) Distribution of group differences in AUC values for node betweenness across 12 networks. MDD: major depressive disorder; HC: healthy control; AUC: area under curve.

FDR corrected) in Network 2 and node betweenness ( $Z = -2.89$ ,  $P = 0.015$ , FDR corrected) in Network 7.

### 3.3 Classification results based on the topological properties of white-matter networks

As shown in Fig. 5, the average accuracy of the classification model based on global topological properties was 56.7% and its classification AUC value was 61.2% (sensitivity=50% and specificity=64%), while the average accuracy on nodal topological properties

was 73.1% and its classification AUC value was 80.3% (sensitivity=72% and specificity=75%).

## 4 Discussion

To the best of our knowledge, this is the first study to map MDD-related individual-level brain WM network changes by using a combination of a wavelet transform method and structural MRI-based brain morphological data. We found that MDD-related



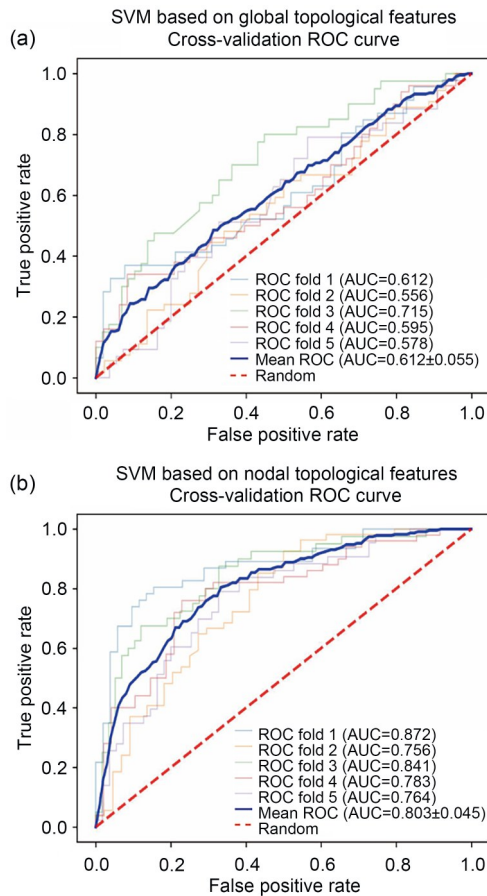


**Fig. 5 Performance evaluation of support vector machine classification.** (a) The ROC curve plotted after SVM classification based on global topological properties (including the ROC curve for each fold and the average ROC curve); (b) The ROC curve plotted after SVM classification based on nodal topological properties (including the ROC curve for each fold and the average ROC curve). AUC: area under the curve; ROC: receiver operating characteristic; SVM: support vector machine.

topological structure changes of the WM network occurred primarily in the sensorimotor superficial WM system. Interregional morphological similarity was first computed to construct a WM network for each participant using 3D wavelet transform based on the WM volume derived from VBM data. Subsequently, the graph theory method was used to characterize the network global and nodal topological abnormalities in MDD. An SVM model based on the nodal topological properties achieved a classification accuracy of 73.1%, which effectively differentiated MDD patients from HCs. These results provide new evidence highlighting the clinical significance of the sensorimotor system and enhancing our understanding of the potential

pathological mechanisms of MDD from the new perspective of WM network.

Our findings demonstrated the distinctive characteristics of morphological similarity or structural connectivity of WM brain networks. These included reduced characteristic path length and increased small-worldness in MDD patients. The observed decrease in  $L_p$  in MDD patients suggested an increased integration capacity within the brain, indicating unusual information transmission. This finding aligns with a previous study reporting similar characteristics in the topological properties of functional brain networks in MDD, which indicated abnormally low  $L_p$  and higher overall efficiency (inversely related to  $L_p$ ). This was explained as a less regularly organized or randomized structure within the WM network (Zhang et al., 2011). Our result on the abnormal small-world properties in MDD is consistent with the previous findings for WM functional networks (Li et al., 2020; Yang et al., 2021). This structural basis of aberrant WM in MDD might be an important factor underlying the wiring patterns of brain networks.

The current study presents new data on the alterations in WM networks associated with MDD. Specifically, the observed elevation in the node degree and node efficiency of the sensorimotor superficial WM system in MDD suggests a heightened level of local interconnectedness and information processing within these regions (Petrella, 2011). This amplified local connectivity might signify a compensatory mechanism or an adaptive response to mitigate disturbances in sensorimotor functions associated with MDD (Luscher et al., 2011). Conversely, the notable reduction in node betweenness within the sensorimotor superficial WM system implies a reduced capacity to act as key intermediaries in information transfer across brain networks (Korgaonkar et al., 2014). This decline in the pivotal role of the WM system might indicate a disrupted flow of information or impaired integration of sensorimotor-related WM tracts in MDD. Significant correlations have been reported between the abnormal topological structure of the sensorimotor WM system and some cognitive scores in MDD (Wang XH et al., 2022). These topological alterations also highlight the intricate network connectivity changes in WM network topologies associated with MDD.

Understanding how the structural connectivity pattern supports and shapes brain function is a fundamental

question in systems neuroscience (Honey et al., 2010). The morphological WM network is optimally organized to support efficient information transmission and processing. Specifically, WM tracts play a crucial role in transmitting sensory and motor information, mediating interhemispheric communication, and connecting various cortical regions (Filley, 1998). It has been suggested that the loss of WM integrity in the frontal lobe might exist across various elder populations and that WM lesions might disrupt neural circuits involved in emotion regulation, involving the neuropathology of MDD (Ma et al., 2007). Our findings suggest that the abnormalities in cognitive control and emotional regulation observed in MDD patients might partly result from shortened information transmission and processing capacity in the sensorimotor network. This may be because the sensorimotor superficial WM system interconnects the default mode, posterior attention, ventral attention, and frontoparietal control networks, suggesting the mediating role of WM networks between these GM network regions across varying distances (Peer et al., 2017). The latter study categorized the organization of WM networks into three tiers, with the superficial WM network significantly correlated with GM networks while the deep network showing relatively less dependence on GM networks. Among these networks, the sensorimotor superficial WM system is a symmetric WM network distributed throughout the entire brain. This further supports the previous notion that superficial WM networks may indirectly interact with GM networks, whereas mid-level and deep WM networks are more likely to communicate directly through axonal interactions (Fan et al., 2020). We tentatively propose that structural topological abnormalities in sensorimotor superficial WM systems might involve the disruption of connections to regions highly associated with cognitive functions, which warrants further investigation.

Using SVM classification models, we further explored whether the topological properties of WM network could serve as potential biomarkers for the clinical identification of MDD patients. Our results showed with 73.1% accuracy that the nodal topological properties of WM networks could effectively distinguish MDD patients from HCs. Previous studies have distinguished MDD and HC with accuracies of 66% (Ramasubbu et al., 2016), 63.7% (Shi et al., 2021), and 73.3% (Nakano et al., 2020) while using the SVM classification model. Another study also found

that the small-world topological properties of the WM functional network can distinguish between unmedicated MDD patients and HC subjects, with an accuracy rate of 76% (Li et al., 2020). Considering the above accuracy rates, the accuracy rate of 73.1% and AUC value of 80.3% in this study essentially constitute a good classification performance and can guide potential clinical applications. In this way, our findings provide supplementary evidence about morphological networks underlying MDD.

The present study has several limitations that need to be addressed. Firstly, previous MDD studies traditionally focused on aberrations in higher-order brain functions, including emotion regulation and attention control. Our findings based on the WM network predominantly center on the abnormalities in primary sensorimotor functions, providing new insights into the pathophysiology of MDD. Meanwhile, further investigating the relationship between WM networks and emotional functions is a meaningful direction. Secondly, common research approaches to characterize WM networks still remain insufficient. Beyond the morphological 3D-wavelet transform method utilized in the present study, there is a further need for the development and refinement of novel research methodologies pertaining to WM.

## 5 Conclusions

In the present study, we detected abnormalities in the sensorimotor superficial WM system of MDD patients, which might serve as new neurobiological markers for this disorder. Moreover, we successfully achieved a good performance based on nodal topological properties of the WM network in distinguishing MDD patients from HCs, providing a valuable reference for clinical research.

## Data availability statement

The dataset of participants is available through a reasonable request to the REST-meta-MDD Consortium (<http://rfmri.org/REST-meta-MDD>).

## Acknowledgments

This work was supported by the Zhejiang Medical and Health Science and Technology Project (No. 2022KY1055), the Zhejiang Provincial Natural Science Foundation of China (No. LY17H180007), the Key Clinical Specialty Construction

Project of Zhejiang Province, and the Key Medical Disciplines of Hangzhou, China.

### Author contributions

Peng WANG, Yang XIAO, and Shaowei XUE designed the research. Peng WANG analyzed data. Yanling BAI drafted the original manuscript. Yanling BAI and Peng WANG edited and revised manuscript. Yuhong ZHENG, Li SUN, Jinhui WANG, and Shaowei XUE reviewed and revised the manuscript. The DIRECT Consortium collected and shared the data. All authors have read and approved the final manuscript, and therefore, have full access to all the data in the study and take responsibility for the integrity and security of the data.

### Compliance with ethics guidelines

Peng WANG, Yanling BAI, Yang XIAO, Yuhong ZHENG, Li SUN, The DIRECT Consortium, Jinhui WANG, and Shaowei XUE declare that they have no conflict of interest.

The research protocols were carried out while following the recommendations of the Helsinki Declaration of Ethical Principles and were approved by the local Institutional Review Board (IRB No. 20201124) in Hangzhou Normal University. All study participants provided written informed IRB-approved consent before participating in the study procedures.

### References

- Alexander-Bloch A, Clasen L, Stockman M, et al., 2016. Subtle in-scanner motion biases automated measurement of brain anatomy from in vivo MRI. *Hum Brain Mapp*, 37(7): 2385-2397.  
<https://doi.org/10.1002/hbm.23180>
- Ashburner J, 2007. A fast diffeomorphic image registration algorithm. *NeuroImage*, 38(1):95-113.  
<https://doi.org/10.1016/j.neuroimage.2007.07.007>
- Aydogan DB, Jacobs R, Dulawa S, et al., 2018. When tractography meets tracer injections: a systematic study of trends and variation sources of diffusion-based connectivity. *Brain Struct Funct*, 223(6):2841-2858.  
<https://doi.org/10.1007/s00429-018-1663-8>
- Bassett DS, Sporns O, 2017. Network neuroscience. *Nat Neurosci*, 20(3):353-364.  
<https://doi.org/10.1038/nn.4502>
- Baum GL, Roalf DR, Cook PA, et al., 2018. The impact of in-scanner head motion on structural connectivity derived from diffusion MRI. *NeuroImage*, 173:275-286.  
<https://doi.org/10.1016/j.neuroimage.2018.02.041>
- Bullmore E, Sporns O, 2012. The economy of brain network organization. *Nat Rev Neurosci*, 13(5):336-349.  
<https://doi.org/10.1038/nn.3214>
- Canbeyli R, 2013. Sensorimotor modulation of mood and depression: in search of an optimal mode of stimulation. *Front Hum Neurosci*, 7:428.  
<https://doi.org/10.3389/fnhum.2013.00428>
- Chen X, Lu B, Li HX, et al., 2022. The direct consortium and the REST-meta-MDD project: towards neuroimaging biomarkers of major depressive disorder. *Psychoradiology*, 2(1):32-42.  
<https://doi.org/10.1093/psyrad/kkac005>
- Fan YS, Li ZH, Duan XJ, et al., 2020. Impaired interactions among white-matter functional networks in antipsychotic-naïve first-episode schizophrenia. *Hum Brain Mapp*, 41(1): 230-240.  
<https://doi.org/10.1002/hbm.24801>
- Fields RD, 2010. Change in the brain's white matter. *Science*, 330(6005):768-769.  
<https://doi.org/10.1126/science.1199139>
- Filley CM, 1998. The behavioral neurology of cerebral white matter. *Neurology*, 50(6):1535-1540.  
<https://doi.org/10.1212/WNL.50.6.1535>
- Fortin JP, Cullen N, Sheline YI, et al., 2018. Harmonization of cortical thickness measurements across scanners and sites. *NeuroImage*, 167:104-120.  
<https://doi.org/10.1016/j.neuroimage.2017.11.024>
- Georgiadis F, Larivière S, Glahn D, et al., 2024. Connectome architecture shapes large-scale cortical alterations in schizophrenia: a worldwide ENIGMA study. *Mol Psychiatry*, 29:1869-1881.  
<https://doi.org/10.1038/s41380-024-02442-7>
- Honey CJ, Thivierge JP, Sporns O, 2010. Can structure predict function in the human brain? *NeuroImage*, 52(3): 766-776.  
<https://doi.org/10.1016/j.neuroimage.2010.01.071>
- Iwabuchi SJ, Krishnadas R, Li CB, et al., 2015. Localized connectivity in depression: a meta-analysis of resting state functional imaging studies. *Neurosci Biobehav Rev*, 51:77-86.  
<https://doi.org/10.1016/j.neubiorev.2015.01.006>
- Korgaonkar MS, Fornito A, Williams LM, et al., 2014. Abnormal structural networks characterize major depressive disorder: a connectome analysis. *Biol Psychiatry*, 76(7): 567-574.  
<https://doi.org/10.1016/j.biopsych.2014.02.018>
- Li HR, Yang J, Yin L, et al., 2021. Alteration of single-subject gray matter networks in major depressed patients with suicidality. *J Magn Reson Imaging*, 54(1):215-224.  
<https://doi.org/10.1002/jmri.27499>
- Li J, Chen H, Fan FY, et al., 2020. White-matter functional topology: a neuromarker for classification and prediction in unmedicated depression. *Transl Psychiat*, 10:365.  
<https://doi.org/10.1038/s41398-020-01053-4>
- Li JL, Li Z, Yang YP, et al., 2023. Morphological brain networks of white matter: mapping, evaluation, characterization, and application. *Adv Sci*, 11(35):e2400061.  
<https://doi.org/10.1002/advs.202400061>
- Liao XH, Vasilakos AV, He Y, 2017. Small-world human brain networks: perspectives and challenges. *Neurosci Biobehav Rev*, 77:286-300.  
<https://doi.org/10.1016/j.neubiorev.2017.03.018>
- Lu FM, Cui Q, Huang XJ, et al., 2020. Anomalous intrinsic connectivity within and between visual and auditory networks in major depressive disorder. *Prog Neuro-Psychopharmacol Biol Psychiatry*, 100:109889.  
<https://doi.org/10.1016/j.pnpbp.2020.109889>

- Luscher B, Shen Q, Sahir N, 2011. The GABAergic deficit hypothesis of major depressive disorder. *Mol Psychiatry*, 16(4):383-406.  
<https://doi.org/10.1038/mp.2010.120>
- Ma N, Li LJ, Shu N, et al., 2007. White matter abnormalities in first-episode, treatment-naive young adults with major depressive disorder. *Am J Psychiatry*, 164(5):823-826.  
<https://doi.org/10.1176/ajp.2007.164.5.823>
- Malhi GS, Mann JJ, 2018. Depression. *Lancet*, 392(10161):2299-2312.  
[https://doi.org/10.1016/s0140-6736\(18\)31948-2](https://doi.org/10.1016/s0140-6736(18)31948-2)
- Maslov S, Sneppen K, 2002. Specificity and stability in topology of protein networks. *Science*, 296(5569):910-913.  
<https://doi.org/10.1126/science.1065103>
- Meinertzhagen IA, 2018. Of what use is connectomics? A personal perspective on the *Drosophila* connectome. *J Exp Biol*, 221(10):jeb164954.  
<https://doi.org/10.1242/jeb.164954>
- Nakano T, Takamura M, Ichikawa N, et al., 2020. Enhancing multi-center generalization of machine learning-based depression diagnosis from resting-state fMRI. *Front Psychiatry*, 11:400.  
<https://doi.org/10.3389/fpsy.2020.00400>
- Pardoe HR, Martin SP, 2022. In-scanner head motion and structural covariance networks. *Hum Brain Mapp*, 43(14):4335-4346.  
<https://doi.org/10.1002/hbm.25957>
- Peer M, Nitzan M, Bick AS, et al., 2017. Evidence for functional networks within the human brain's white matter. *J Neurosci*, 37(27):6394-6407.  
<https://doi.org/10.1523/JNEUROSCI.3872-16.2017>
- Petersen SE, Sporns O, 2015. Brain networks and cognitive architectures. *Neuron*, 88(1):207-219.  
<https://doi.org/10.1016/j.neuron.2015.09.027>
- Petrella JR, 2011. Use of graph theory to evaluate brain networks: a clinical tool for a small world? *Radiology*, 259(2):317-320.  
<https://doi.org/10.1148/radiol.11110380>
- Power JD, Cohen AL, Nelson SM, et al., 2011. Functional network organization of the human brain. *Neuron*, 72(4):665-678.  
<https://doi.org/10.1016/j.neuron.2011.09.006>
- Ramasubbu R, Brown MRG, Cortese F, et al., 2016. Accuracy of automated classification of major depressive disorder as a function of symptom severity. *NeuroImage Clin*, 12:320-331.  
<https://doi.org/10.1016/j.nicl.2016.07.012>
- Sampaio-Baptista C, Johansen-Berg H, 2017. White matter plasticity in the adult brain. *Neuron*, 96(6):1239-1251.  
<https://doi.org/10.1016/j.neuron.2017.11.026>
- Schilling KG, Gao YR, Stepniewska I, et al., 2019. Anatomical accuracy of standard-practice tractography algorithms in the motor system – a histological validation in the squirrel monkey brain. *Magn Reson Imaging*, 55:7-25.  
<https://doi.org/10.1016/j.mri.2018.09.004>
- Seidlitz J, Váša F, Shinn M, et al., 2018. Morphometric similarity networks detect microscale cortical organization and predict inter-individual cognitive variation. *Neuron*, 97(1):231-247.e7.  
<https://doi.org/10.1016/j.neuron.2017.11.039>
- Shi YC, Zhang LH, Wang Z, et al., 2021. Multivariate machine learning analyses in identification of major depressive disorder using resting-state functional connectivity: a multi-central study. *ACS Chem Neurosci*, 12(15):2878-2886.  
<https://doi.org/10.1021/acscchemneuro.1c00256>
- Wang JH, Wang XD, Xia MR, et al., 2015. GREYNA: a graph theoretical network analysis toolbox for imaging connectomics. *Front Hum Neurosci*, 9:386.  
<https://doi.org/10.3389/fnhum.2015.00386>
- Wang P, Wang JL, Michael A, et al., 2022. White matter functional connectivity in resting-state fMRI: robustness, reliability, and relationships to gray matter. *Cereb Cortex*, 32(8):1547-1559.  
<https://doi.org/10.1093/cercor/bhab181>
- Wang XH, Zhao BH, Li LH, 2022. Mapping white matter structural covariance connectivity for single subject using wavelet transform with T1-weighted anatomical brain MRI. *Front Neurosci*, 16:1038514.  
<https://doi.org/10.3389/fnins.2022.1038514>
- Wang Y, Liu G, Hong DD, et al., 2016. White matter injury in ischemic stroke. *Prog Neurobiol*, 141:45-60.  
<https://doi.org/10.1016/j.pneurobio.2016.04.005>
- Whitwell JL, 2009. Voxel-based morphometry: an automated technique for assessing structural changes in the brain. *J Neurosci*, 29(31):9661-9664.  
<https://doi.org/10.1523/jneurosci.2160-09.2009>
- Xiao Y, Zhao L, Zang XL, et al., 2023. Compressed primary-to-transmodal gradient is accompanied with subcortical alterations and linked to neurotransmitters and cellular signatures in major depressive disorder. *Hum Brain Mapp*, 44(17):5919-5935.  
<https://doi.org/10.1002/hbm.26485>
- Yan CG, Chen X, Li L, et al., 2019. Reduced default mode network functional connectivity in patients with recurrent major depressive disorder. *Proc Natl Acad Sci USA*, 116(18):9078-9083.  
<https://doi.org/10.1073/pnas.1900390116>
- Yang H, Chen X, Chen ZB, et al., 2021. Disrupted intrinsic functional brain topology in patients with major depressive disorder. *Mol Psychiatry*, 26(12):7363-7371.  
<https://doi.org/10.1038/s41380-021-01247-2>
- Yeo BTT, Krienen FM, Sepulcre J, et al., 2011. The organization of the human cerebral cortex estimated by intrinsic functional connectivity. *J Neurophysiol*, 106(3):1125-1165.  
<https://doi.org/10.1152/jn.00338.2011>
- Zalesky A, Fornito A, Harding IH, et al., 2010. Whole-brain anatomical networks: does the choice of nodes matter? *NeuroImage*, 50(3):970-983.  
<https://doi.org/10.1016/j.neuroimage.2009.12.027>
- Zhang FF, Peng W, Sweeney JA, et al., 2018. Brain structure alterations in depression: psychoradiological evidence. *CNS Neurosci Ther*, 24(11):994-1003.  
<https://doi.org/10.1111/cns.12835>
- Zhang YR, Liu XY, Hou ZH, et al., 2021. Global topology alteration of the brain functional network affects the 8-week antidepressant response in major depressive disorder. *J*



- Affect Disord*, 294:491-496.  
<https://doi.org/10.1016/j.jad.2021.07.078>
- Zhang ZQ, Liao W, Chen HF, et al., 2011. Altered functional–structural coupling of large-scale brain networks in idiopathic generalized epilepsy. *Brain*, 134(10):2912-2928.  
<https://doi.org/10.1093/brain/awr223>
- Zhou Y, Zhu YH, Ye HT, et al., 2024. Abnormal changes of dynamic topological characteristics in patients with major depressive disorder. *J Affect Disord*, 345:349-357.  
<https://doi.org/10.1016/j.jad.2023.10.143>